Magnetic Resonance Imaging 31 (2013) 1752–1759

Contents lists available at ScienceDirect

Magnetic Resonance Imaging

journal homepage: www.mrijournal.com

Technical notes

Fast and high-resolution quantitative mapping of tissue water content with full brain coverage for clinically-driven studies☆,☆☆

Mohammad Sabati *, Andrew A. Maudsley

Department of Radiology, Miller School of Medicine, University of Miami, Miami, FL 33136

ARTICLE INFO

Article history:
Received 31 May 2013
Revised 15 July 2013
Accepted 2 August 2013

Keywords:
Quantitative MRI
Water content mapping
T1 mapping
Dual-angle acquisition
SPGR sequence
RF nonuniformity
Reproducibility

ABSTRACT

An efficient method for obtaining longitudinal relaxation time (T1) maps is based on acquiring two spoiled gradient recalled echo (SPGR) images in steady states with different flip angles, which has also been extended, with additional acquisitions, to obtain a tissue water content (M0) map. Several factors, including inhomogeneities of the radio-frequency (RF) fields and low signal-to-noise ratios may negatively affect the accuracy of this method and produce systematic errors in T1 and M0 estimations. Thus far, these limitations have been addressed by using additional measurements and applying suitable corrections; however, the concomitant increase in scan time is undesirable for clinical studies. In this note, a modified dual-acquisition SPGR method based on an optimization of the sequence formulism is presented for good and reliable M0 mapping with an isotropic spatial resolution of $1 \times 1 \times 1$ mm^3 that covers the entire human brain in 6:30 min. A combined RF transmit/receive map is estimated from one of the SPGR scans and the optimal flip angles for M0 map are found analytically. The method was successfully evaluated in eight healthy subjects producing mean M0 values of 69.8% (in white matter) and 80.1% (in gray matter) that are in good agreement with those found in the literature and with high reproducibility. The mean value of the resultant voxel-based coefficients-of-variation was 3.6%.

1. Introduction

Quantitative MR techniques are of interest in human brain imaging as methods for increasing sensitivity for detection of tissue pathologies. In particular, non-invasive mapping of the tissue water content, M0, in the human brain has been shown to be of value in areas such as brain cancer [1], chronic alcoholism [2], multiple sclerosis [3], ischemia [4], and hepatic encephalopathy [5]. Many pathological conditions are accompanied by a diffuse or global increase in water content [6,7], but which may not be detectable with a high specificity by non-quantitative imaging methods [8]. It therefore would be very useful to determine the magnitude and extent of the changes in water concentration.

Although a number of M0 mapping methods have been recently developed [9–13] and applied to studies in human brain, scan times tend to be long and therefore reductions in acquisition times are desirable for routine clinical use. In addition to rapid acquisition, many other factors, such as high sensitivity, high reproducibility, high isotropic resolution, and good image contrast determine the selection of the M0 mapping methods. Usually, quantitative water measurement of brain tissues requires extra acquisitions and calibrations than those used for longitudinal relaxation time, T1, mapping and is more challenging. Neeb et al. [10,14] have combined T1 mapping with partial inversion recovery with another multi-slice and multi-time point sequence for T2* mapping, and acquired three extra data sets to correct for local radio-frequency (RF) transmit field, B_1^+, variation, temperature differences between the subject and a reference probe placed in the field-of-view (FOV), receiver profile inhomogeneities, B_1^-, and T1 saturation effects. This approach resulted in accurate quantitative M0 maps, though it required several processing and corrections steps and a lengthy overall scan time which is less suitable when scanning patients. Warntjes et al. [13] presented another method for simultaneous quantitation of T1, T2* and water density. Using a double-echo saturation recovery-SPGR approach, full brain water content maps were acquired with a resolution of $1 \times 1 \times 1.5$ mm^3 at 1.5 T in about eight minutes. However, measuring T2* using two points with different echo times (TE) in their approach makes the determination of water content sensitive to magnetic field inhomogeneities. Also, the reference measurement was determined in a separate scan, potentially compromising accuracy.

☆ Portions of this work were presented at the 18th and the 19th Scientific Meetings of the International Society for Magnetic Resonance in Medicine in Stockholm, Sweden (1–7 May 2010) and Montreal, QC, Canada (7–13 May 2011), respectively.

☆☆ Grant Sponsor: National Institutes of Health (Grant number: R01EB000822).

* Corresponding author. Department of Radiology, Miller School of Medicine, University of Miami, 1150 NW 14 Street, Suite 713, Miami, FL 33136. Tel.: +1 305 243 7458; fax: +1 305 243 3405.
E-mail address: msabati@med.miami.edu (M. Sabati).

0730-725X/$ – see front matter © 2013 Elsevier Inc. All rights reserved.
http://dx.doi.org/10.1016/j.mri.2013.08.001

An efficient method for obtaining M0 maps through T1 mapping is based on acquiring two SPGR images in steady-states with different flip angles [11,15,16]. However, several factors, including B_1^+ and B_1^-, particularly at higher field strengths [17], T1 saturation, and low SNR may negatively affect the accuracy of these methods and produce systematic errors in M0 estimation when such T1-dependent methods are used. In a recent study, Volz et al. [11] applied an SNR-optimized, dual-angle, SPGR-based T1 mapping method [16], with necessary corrections, to map M0 at 1-mm isotropic resolution in 18 min. The intensity-corrected images were converted into quantitative M0 maps by normalizing to a reference signal obtained from a cerebrospinal fluid (CSF) region, assuming a value of 100% water [18].

In this study, a modified two-acquisition SPGR method is presented for M0 mapping. Linear parameterization is used to independently estimate the brain tissue T1 and M0 values. The two flip angles for optimal T1 mapping (*i.e.*, with maximum SNR) were previously found both numerically [15] and analytically [16], although it is demonstrated here that these are not optimal for M0 mapping. Therefore, the optimal flip angles for SNR-optimized M0 maps are analytically derived and results are verified in eight normal subjects on a 3.0 T clinical scanner. It is demonstrated that correct and reliable M0 maps can be obtained with an isotropic resolution of 1 mm that covers the entire human brain in a clinically acceptable scan time of 6:30 min using only two acquisitions.

2. Theory

The variable flip angle SPGR approach for T1 and M0 mapping is based on the dependence of the steady-state signal on the flip angle α, the repetition time TR, the echo time TE, and the proton density, given by:

$$S = K.B_1^-.M_0 \cdot \frac{1-e^{-TR/T_1}}{1-\cos\left(B_1^+\alpha\right)\cdot e^{-TR/T_1}} \cdot \sin\left(B_1^+\alpha\right)\cdot e^{-TE/T_2^*}, \quad [1]$$

where M0 is the equilibrium magnetization directly proportional to the voxel water content, B_1^+ is the actual-to-nominal flip angle ratio (ideally equals to 1.0), B_1^- is the receiver coil profile, and K is a constant. A plot of $S/\sin(B_1^+\alpha)$ versus $S/\tan(B_1^+\alpha)$ yields a straight line of $S/\sin(B_1^+\alpha) = m.[S/\tan(B_1^+\alpha)] + b$ where T1 can be determined from the slope $m = \exp(-TR/T1)$ while M0 can be determined from $b/(1-m)$. SNR calculation and optimization of flip angles have been previously studied for T1 mapping [15,16]. Here, the focus is on the determination of these parameters for M0 mapping. Without loss of generality, $B_1^+ = 1.0$ and $B_1^- = 1.0$ are assumed for the following calculations and their effects are then applied at later steps.

Following a similar approach of Preibisch and Deichmann [16], if only two acquisitions with flip angles α_1 and α_2 (*i.e.*, producing S_1 and S_2 SPGR signals) are performed, KM_0E^* can be calculated from linearization of Eq. [1] by [19]:

$$KM_0E^* = \frac{b}{1-m} = \frac{AS_1S_2}{BS_2 - CS_1} \quad [2]$$

where $E^* = \exp(-TE/T_2^*)$, and

$$\begin{aligned} A &= \sin(\alpha_2)\tan(\alpha_1) - \sin(\alpha_1)\tan(\alpha_2), \\ B &= \tan(\alpha_1)\sin(\alpha_1)(\sin(\alpha_2) - \tan(\alpha_2)), \\ C &= \tan(\alpha_2)\sin(\alpha_2)(\sin(\alpha_1) - \tan(\alpha_1)). \end{aligned} \quad [3]$$

Provided that the two measurements S_1 and S_2 are performed with the same bandwidth and receiver gain, the noise level σ_s is the same in both images. The noise in the M0 map is then given by:

$$\sigma_{M_0} = \sqrt{\left(\frac{\partial M_0}{\partial S_1}\right)^2 + \left(\frac{\partial M_0}{\partial S_2}\right)^2}\,\sigma_s \quad [4]$$

The partial derivatives can be calculated from Eqs. [2] and [3]:

$$\frac{\partial M_0}{\partial S_1} = \frac{ABS_2^2}{KE^*(BS_2 - CS_1)^2}, \frac{\partial M_0}{\partial S_2} = -\frac{ACS_1^2}{KE^*(BS_2 - CS_1)^2} \quad [5]$$

Replacing these expressions into Eq. [4] yields:

$$\sigma_{M_0} = A\frac{\sqrt{B^2S_2^4 + C^2S_1^4}}{KE^*(BS_2 - CS_1)^2}\sigma_s \quad [6]$$

To maximize the SNR in the M0 map, the pair of flip angles (α_1, α_2) that minimizes Eq. [6] for a given TR value can be found numerically as shown in Fig. 1 where the dotted vertical line corresponds to the TR value used in this study. Although the exact localization of the minimum depends on T1 (via S_1 and S_2), the minima are broad and the range of T1 values in the human brain tissue is sufficiently small (gray matter ~1400 ms, white matter ~900 ms at 3.0 T) [20]. Thus, the optimum flip angles are chiefly TR-dependent and for the TR used in this work were determined for an intermediate T1 of 1100 ms. Note, however, that the nominal M0 map is calculated directly from the measured SPGR signals S_1 and S_2, and the flip angles only (see Eq. [2]), independent of T1 calculations.

As shown by Helms et al. [21], for TR/T1 ≪ 1 and α < 40° (*c.f.* Fig. 1 of Ref. [21]), the influence of the flip angle miscalibration, B_1^+, and the receiver coil profile, B_1^-, on the estimated T1 and M0 parameters from the nominal flip angles can be approximated as:

$$\mathrm{T1}_{nom} = \mathrm{T1}\,B_1^{+2}, \mathrm{M0}_{nom} = \mathrm{M0}\,B_1^+\,B_1^- \quad [7]$$

Thus, when using the proton-density-weighted SPGR signal as a measure for RF coils homogeneity, the effects of excitation and reception are confounded.

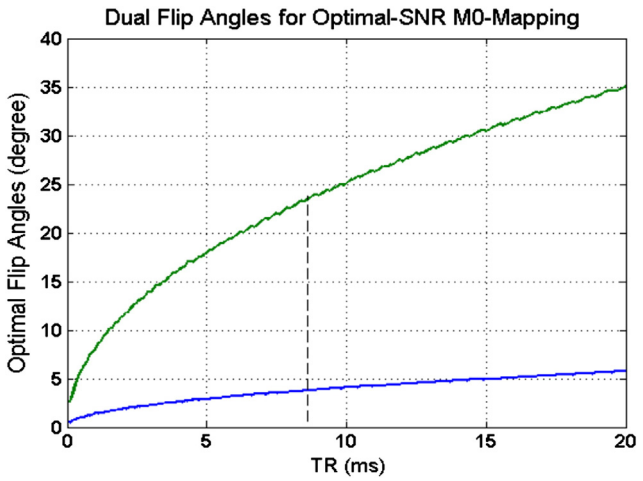

Fig.1. Optimal flip angles as a function of TR to obtain maximum-SNR for M0 mapping using dual SPGR-acquistion obtained by numerical solution of Eq. [6]. T1 = 1100 ms was assumed. Notice that one small flip angle (<6°) (shown in blue) is favorably yielded for short TR, for which sin(α) can be approximated with α so that the related SPGR image can be used for a combined $B_1^- \cdot B_1^+$ estimate after appropriate processing (see text). The dotted vertical line corresponds to the TR value used in this study (*i.e.*, TR = 8.4 ms). The green curve represents the larger yielded optimal flip angle.

3. Materials and methods

All measurements were performed at 3.0 T (Magnetom Trio/TIM, Siemens Medical Solutions, Erlangen, Germany) using an 8-channel phased-array receive-only head coil (In Vivo Corp., Waukesha, WI, USA) and a whole-body transmit coil. Eight healthy subjects (5 male, 3 female, age: 27.3 ± 2.6 years, age range: 22–30 years) were scanned. The study was approved by the local Institutional Review Board and written consent was obtained from all participants.

The mathematical framework presented above gives rise to a small flip angle (<6°) for relatively small TR's (<20 ms) for which the steady-state SPGR signal S can be approximated by [22–24]:

$$S \propto K B_1^- M_0 \cdot \sin\left(B_1^+ \alpha\right).e^{-TE/T_2^*} \propto K M_0 B_1^- B_1^+ \alpha.e^{-TE/T_2^*}, \quad [8]$$

where $B_1^- \cdot B_1^+ \stackrel{def}{=} B_1$ represents a combined RF transmit and receive coil nonuniformities. For small angles, it is unlikely that coherences of residual transverse magnetization occur, so S can be assumed to be similar to theoretical SPGR signal of Eq. [1]. Thus, when using a proton-density-weighted with a small flip angle SPGR signal as a measure for RF inhomogeneities, the effects of excitation and reception are combined, as in Eq. [7] [21]. Because B_1 is a spatially smooth function; e^{-TE/T_2^*} is spatially invariant at small TE ($\ll T_2^*$); and M0 exhibits low image contrast, a B_1 map can be approximated by heavily smoothing the small-flip angle SPGR signal; and then applied to the initial $M0_{nom}$ estimate for correction [23]. Notice, that it is unnecessary to assume $B_1^- \approx B_1^+$ based on the reciprocity theorem. To create the reference B_1 map, the small-flip angle SPGR signal was first smoothed using convolution with a $5 \times 5 \times 5$ Hanning kernel for fifteen times. It was found that in most cases the B_1 map monotonically reaches steady state values after ten smoothing steps and changes were negligible thereafter. A fewer smoothing steps would retain rapid spatial variations that may be present on the small flip angle SPGR image; and it is therefore not recommended. Then, the "mean" of the resultant 3D map was normalized to 1.0 as an estimate for the B_1 map; (practically, it is assumed that the RF excitation and detection process on a MR instrument would target an ideal and spatially-uniform RF profile). Thus, provided the B1 profile is known, M0 can be obtained from $M0_{nom}$ according to Eq. [7] while choosing the scaling constant K in a way that M0 achieves a value of 100% in CSF [18]. The second SPGR data set (with the larger flip angle) was used for brain extraction and tissue segmentation, respectively, by using the brain extraction tool (BET) [25] and the segmentation tool (FAST) [26] of the FSL software (FMRIB, University of Oxford, UK). A brain mask was applied on the low-flip angle data after the smoothing process and followed by B1 normalization.

Four variable-flip angle SPGR scans with the following parameters were used: TR/minTE = 8.4/3.76 ms, flip angles: 4°, 15°, 23°, and 27°, acquisition matrix = 256 × 256, BW = 210 Hz/Px, FOV = 256 × 256 mm^2, 160 slices, 1-mm slice thickness, no gap between slices, iPAT acceleration factor = 2 with 24 auto-calibration lines, and total acquisition time of 3 min and 14 s per scan. Three pairs of SPGR scans with flip angles (a) $\alpha1 = 4°$, $\alpha2 = 15°$ (optimal flip angles for T1 mapping based on scan parameters, *c.f.* Refs. [15,16]) (b) $\alpha1 = 4°$, $\alpha2 = 23°$ (optimal flip angles for M0 mapping, see Theory and Fig. 1), and (c) $\alpha1 = 4°$, $\alpha2 = 27°$ (mildly larger than the optimal flip angle) were used for maps reconstructions. These were compared to maps obtained using all four scans by linear least squares estimation (referred to as a reference map: M0-Ref). T1 in CSF was limited to 4500 ms [13] and M0 values were normalized to the mean M0 value of the CSF in the ventricles only; assuming a constant water concentration of 100% [18,27,28]. The ventricles were delineated by applying a threshold on the segmented CSF image (obtained from FAST) followed by a center-of-mass algorithm. M0 maps were spatially transformed to a common reference space (MNI; Montreal Neurological Institute) and mean values in eight atlas-defined brain regions (*i.e.*, left and right frontal, temporal, parietal, and occipital lobes) were calculated for each subject, using the four different flip angles combinations mentioned above. To assess the spatial variations of the proposed M0 method, two experiments were conducted in a large cylindrical phantom filled with gadolinium-doped 100% water at two different concentrations. The targeted relaxation times (T1/T2) for the experiments were approximately 1000 ms/716 ms and 700 ms/522 ms. Mean and standard deviation as well as in-plane and through-plane profile measurements were performed on the final phantom M0 images.

To verify the reproducibility of the M0 mapping, two subjects, one 26-year-old female and one 29-year-old male, were scanned at five separate occasions at approximately weekly intervals. Using all studies from each subject, a voxel-based analysis of the M0 images was applied to determine the mean and standard deviation at each location. Maps of the coefficients of variance (COV), in percent, at each voxel were then generated, and these results from two subjects were then combined to determine the distributions of COVs.

4. Results

In Fig. 1 are shown the optimal dual flip angles, found numerically, as functions of TR that minimizes Eq. [6] (*i.e.*, maximizing the SNR in M0 mapping) where the dotted vertical line corresponds to the TR = 8.4 ms used in this study yielding to flip angles of 4° and 23°. Note that α_1 increases slowly with TR and remains small (< 6°) for short TR. Fig. 2 illustrates a representative

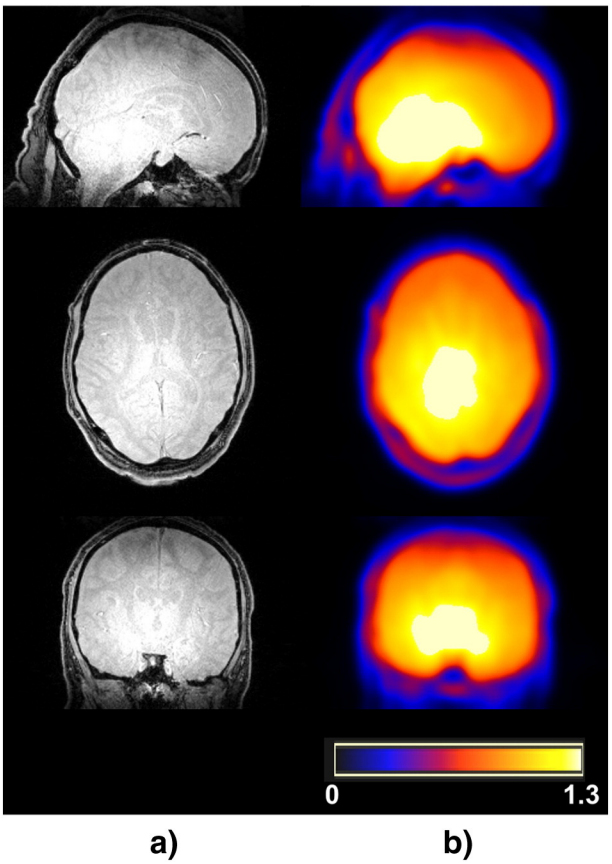

Fig. 2. (a) Representative original SPGR images with small flip angle ($\alpha = 4°$) linearly affected by the nonuniformity of the radio frequency B_1^+ and B_1^- profiles. (b) 3D combined transmit/receive B1 map estimated by heavy smoothing of (a) and normalization to 1.0. Color map range: 0.54–1.27 within the brain.

3D small-flip angle SPGR image and the estimated 3D transmit/receive B1 map in three orthogonal planes. The color map represents a wide B1 range of 0.54–1.27 in the whole brain. It is noted that B1 estimate may no longer be accurate in cases of pathology where severe hypo or hyper intense regions may present on the low flip angle SPGR image. Fig. 3 shows B1-corrected M0 map from a phantom experiment (T1/T2 ~ 1000 ms/716 ms) at three orthogonal planes demonstrating homogenous images and uniform in-plane and through-plane profiles within most of the central volume. However, high M0 values at the perimeter of the phantom are apparent owing to the suboptimal B1 estimate at the periphery, where small B1 values have inflated M0 (see Eq. [7]). Also, note the through-slice profile at the edges of imaged volume due to the sequence 3D slab excitation profile. Similar results were obtained from the phantom experiment with targeted T1/T2 ~ 700 ms/522 ms. Within the central 75% of the entire volume, the M0 standard deviations for the two phantom experiments were 1.1% and 0.9% of the M0 mean value (*i.e.*, 100% water). In Fig. 4 are shown the estimated B1, uncorrected T1 and the corrected M0 quantitative maps at a middle slice obtained from two subjects with (top row) and without (bottom row) scanner-provided receiver coil, B_1^-, calibration. Uncorrected M0 maps with high B1-nonunformity manifestations are also shown for comparison. In both cases, the B1 maps were properly estimated and correct M0 value obtained throughout the brain. In Fig. 5 are shown five representative slices of a 22-year-old male subject demonstrating the capability of obtaining T1 and M0 maps with full brain coverage and excellent quality, although the T1 maps are not quantitatively corrected. However, noticeably bright pixels on the perimeter of the brain are projected originating from the low SPGR signals of the skull and the suboptimal B1 estimate at the brain boundaries, where small B1 values have inflated M0 (see Eq. [7]).

In Fig. 6 are shown M0 maps from a 26-year-old male subject using four flip-angle combinations. The whole-brain white and gray matters, (WM, GM), M0 values for the (4°, 15°), (4°, 23°), and (4°, 27°) pairs were (67.3%, 76.0%), (69.3%, 79.6%), and (66.5%, 74.9%), respectively, compared to (70.2%, 79.7%) of the M0-Ref (WM, GM) measures. The pair (4°, 23°) M0 map (Fig. 6b) demonstrates the smallest difference to the M0-Ref map with normalized root-mean-square error (RMSE) value of 1.6%, supporting the analytical solution of Eq. [6]. RMSE values for (4°, 15°) and (4°, 27°) pairs were 2.9% and 5.5%, respectively. These results confirm that the optimal flip angle pair of (4°, 23°) estimated the water content more accurately as indicated by agreement with the M0-Ref and the values found in literature [9,11,13,14]. Other flip-angle combinations generally underestimated the tissue M0 values. The RMSE for all subjects ranged from 1.3% to 4.7% for the (4°, 23°)-pair whereas it ranged from 2.9% to 7.6% for the (4°, 15°)-pair. Mean M0 values for each of the eight atlas-defined brain regions and tissue type from all normal subjects are given in Table 1. The mean whole-brain WM and GM water contents across the group of subjects resulted in values of 69.8% ± 2.4% and 80.1% ± 2.1%, respectively; and are consistent with previous studies [9,11,13,14].

In Fig. 7 are shown example M0 images from a 26-year-old female, with selected axial slices from a single study, the mean-value M0 image generated by summation over five repeated studies, and the resultant COV image, which has been displayed with an image scale between 0% and 10%. COV values from the voxel-based analysis throughout the whole brain resulted in 2.7% ± 1.1%, 3.9% ± 1.3%, and 5.2% ± 1.3% for the WM, GM, and CSF, respectively. The M0 COV image showed lower values in the tissue (particularly, central white-matter), which is indicative of the relatively more robust estimation of the RF field nonuniformity in these regions. The overall mean value for the voxel-based COV's of the M0 image in the brain tissue was 3.6%, lending support to the use of this approach for providing a reliable water content measure for longitudinal studies; however, it is noted that this result may no longer apply in cases of pathology.

The COVs from the lobar-scale region analysis for the GM, WM, and CSF M0 values were 1.3%, 1.7%, and 1.8%, respectively. These values were derived from the tissue segmentation analysis, and the average value obtained by integration over all voxels within the whole cerebrum of the two subjects. COVs for the region-based

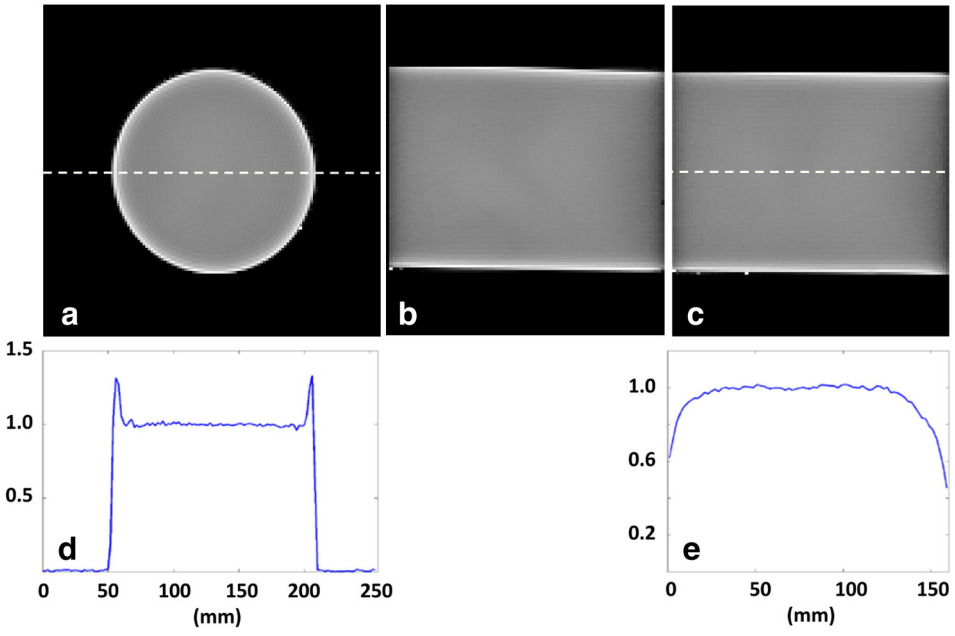

Fig. 3. (a–c) Representative three orthogonal M0 images obtained from a homogenous, cylindrical phantom filled with 100% gadolinium-doped water (targeted T1/T2 ~ 1000 ms/716 ms) showing homogenous maps and uniform (d) in-plane and (e) through-plane profiles (at dashed lines) within most of the central volume. High M0 values are apparent at the periphery while low M0 values are present at the edges of imaged volume (see text). M0 standard deviation was only 1.1% (of the M0 mean value) within the central 75% of the entire volume. Image contrast and brightness are adjusted for better visualization of M0 variations.

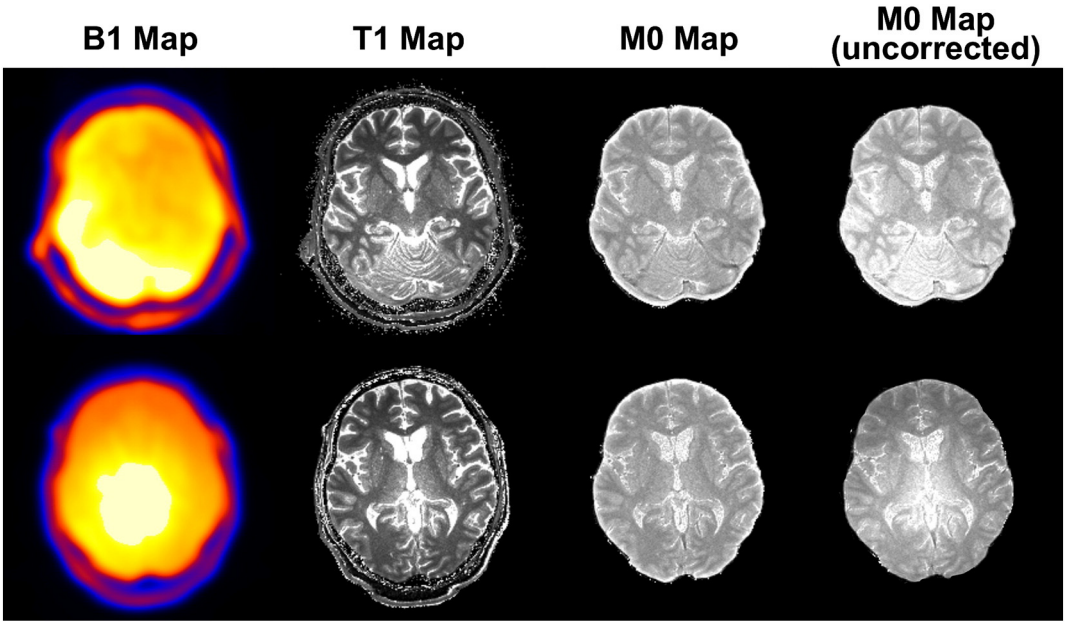

Fig. 4. Representative 1-mm isotropic resolution slices of the estimated B1 and the T1 (uncorrected) and water content M0 maps from two subjects with (top row) and without (bottom row) scanner-provided receiver coil B_1^- correction obtained by using the (4°, 23°)-flip angle pair. Excellent-quality maps were obtained. Uncorrected water content maps with clear B1-nonuniformity evident are also shown for comparison. M0 values were normalized to CSF M0 values, assuming 100% water concentration.

measurements were significantly less than the corresponding mean values obtained from the voxel-based analysis, illustrating the increased potential for detection of subtle water alterations following integration over larger brain regions.

5. Discussion

Accurate mapping of tissue water content with high spatial resolution and short data acquisition times is technically challenging [11,14]. This study has demonstrated that the previously-published method for T1 mapping based on two rapidly-acquired images with different flip angles can be modified to use optimized flip angles for M0 mapping in human brain at 3.0 T. The M0 mapping approach proposed by Neeb et al. [14], based on multiple acquisitions, produced an error of <5% in the water measurement for a single voxel at 1.5 T. However, the concomitant increase in scan time and the examination preparations render the technique intractable in a clinical environment and also more susceptible to subject motion. Volz et al. [11] investigated the accuracy of M0 mapping using an optimized T1 mapping method [16] along with additional T2* and B_1^+ mapping and a bias field correction for receiver coil sensitivity. It was found that the bias field corrections [23] produced more reliable M0 maps than using RF transmit/receive reciprocity principle. Although 1-mm isotropic resolution maps with comparable results to literature values [9,10,13,14] (*c.f.* Table 1 of Ref. [11]) were obtained, the overall 18 min scan time is still a concern when scanning patients.

The method presented in this study corrects for most of the abovementioned effects by finding optimal excitation angles, appropriate acquisition parameters, a compound B1 map estimate,

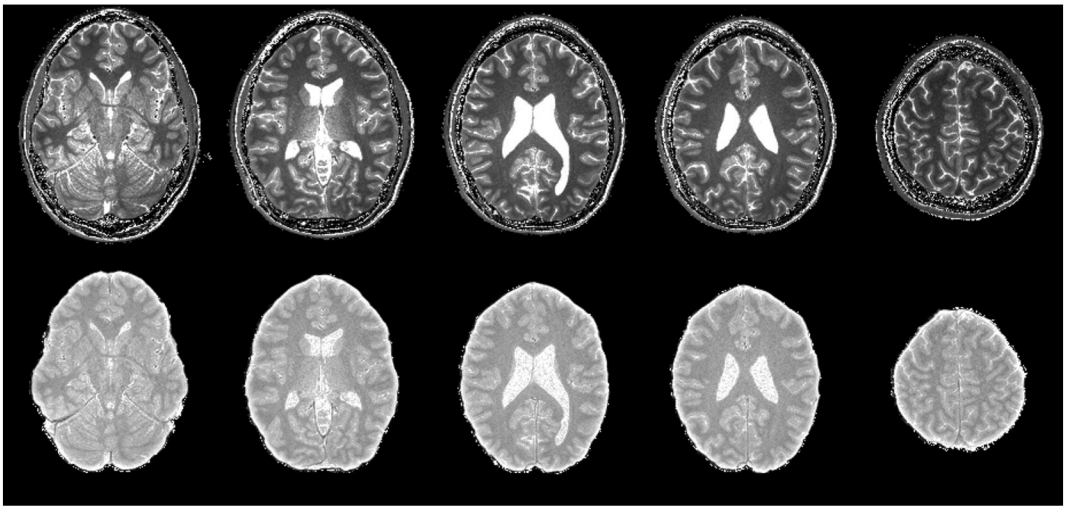

Fig. 5. Five representative 1-mm isotropic resolution slices of the estimated T1 maps (0–3000 ms) (top row) and water content M0 maps (0%–100%) (bottom row) obtained from whole-brain of a 22-year-old male subject. M0 values were corrected for B1-nonuniformity and normalized to pure CSF M0 value, assuming 100% water concentration. For better visualization, CSF T1 values were clipped to 3000 ms level.

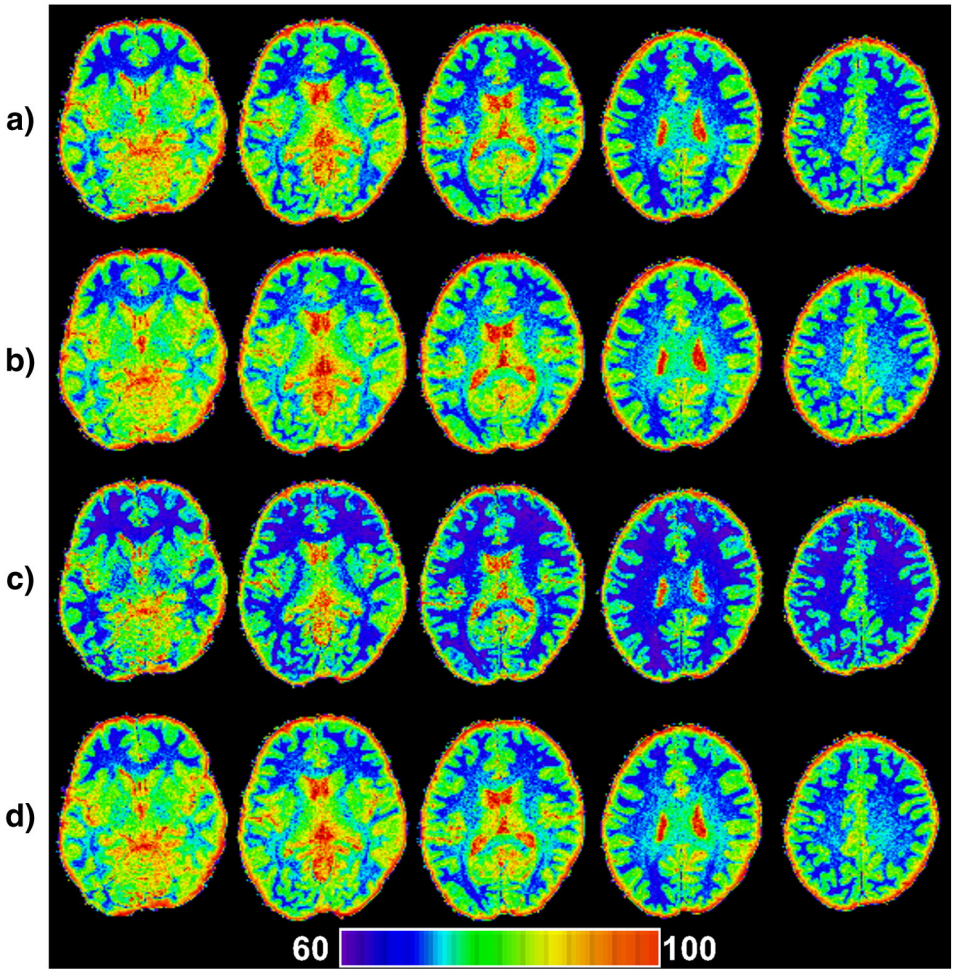

Fig. 6. Representative high-resolution images of the B1-corrected M0 maps, obtained with (a) (4°, 15°); (b) (4°, 23°); (c) (4°, 27°); and (d) (4°, 15°, 23°, 27°) acquisitions. The (4°, 15°)-pair SPGR scans (optimal flip angles for T1 mapping) and (4°, 27°)-pair resulted in underestimation of the M0 values compared to the M0-Ref map of (d). For (a), (b), and (c), the RMSE values relative to the M0-Ref map of (d) were 2.9%, 1.6%, and 5.5%, respectively.

and by using an internal reference of the pure CSF water concentration [18,27,28]. This study shows that despite the complication caused by RF excitation and detection nonuniformity (Fig. 2), the results (Table 1) attain a precision for M0 estimation that is comparable to previous reports [9,11,13,14], yet in a shorter scan time and at high spatial resolution. Furthermore, the high reproducibility of the M0 signal through COV calculations is supporting the use of this method for pre and post treatment studies. Due to its volumetric and high SNR, and post-processed B1 estimation, the proposed method can potentially provide fast, efficient, and high-quality maps of the brain tissue T1 and M0 simultaneously at lower static field where B_1^+ nonuniformity is of less concern. Also, the post-processing steps of the proposed approach are straightforward and can be incorporated into online reconstruction. However, it should be noted that B1 estimates may no longer be accurate in cases of pathology such as brain tumors or lesions where considerable hypo or hyper intense regions may present on the low flip angle SPGR image.

Published values for the T1 relaxation time of brain tissues vary over a large range [9,10,15,16,29–35]. It has been shown that the

Table 1
Mean M0 values normalized to 100% water content in each brain region and GM and WM tissue from eight normal subjects (age: 22–30 years).

Brain region	Frontal		Temporal		Parietal		Occipital	
Brain tissue	L	R	L	R	L	R	L	R
Gray Matter								
M0-Ref	78.9 ± 1.9	80.0 ± 1.6	81.2 ± 1.8	80.9 ± 2.0	78.0 ± 1.8	77.5 ± 1.3	80.5 ± 1.7	81.3 ± 1.5
M0-(4°, 23°)	79.2 ± 2.0	80.7 ± 1.5	80.9 ± 2.2	81.1 ± 1.8	78.4 ± 2.4	77.7 ± 1.5	79.8 ± 1.4	80.6 ± 1.6
M0-(4°, 15°)	76.5 ± 2.8	77.2 ± 2.1	76.1 ± 3.0	76.8 ± 2.7	73.9 ± 2.4	75.0 ± 2.1	75.2 ± 1.9	76.8 ± 1.8
White Matter								
M0-Ref	69.5 ± 1.7	68.9 ± 2.0	71.9 ± 1.7	71.3 ± 1.4	68.2 ± 1.5	68.4 ± 1.7	70.0 ± 1.2	70.2 ± 1.1
M0-(4°, 23°)	69.0 ± 1.6	69.3 ± 1.9	70.9 ± 1.3	71.0 ± 1.8	68.6 ± 1.7	67.9 ± 2.1	68.6 ± 1.9	70.5 ± 1.6
M0-(4°, 15°)	66.5 ± 1.8	67.1 ± 2.2	68.0 ± 1.6	68.9 ± 1.7	66.2 ± 1.8	65.8 ± 1.9	67.1 ± 2.2	67.9 ± 1.9

M0-Ref represents the reference water content estimate using the least squares linearization of all four SPGR scans with variable flip angles of 4°, 15°, 23°, and 27°. Notice that the (4°, 23°) dual acquisitions generated the closest results to the M0-Ref and had the smallest RMS error compared to other flip angle pairs.

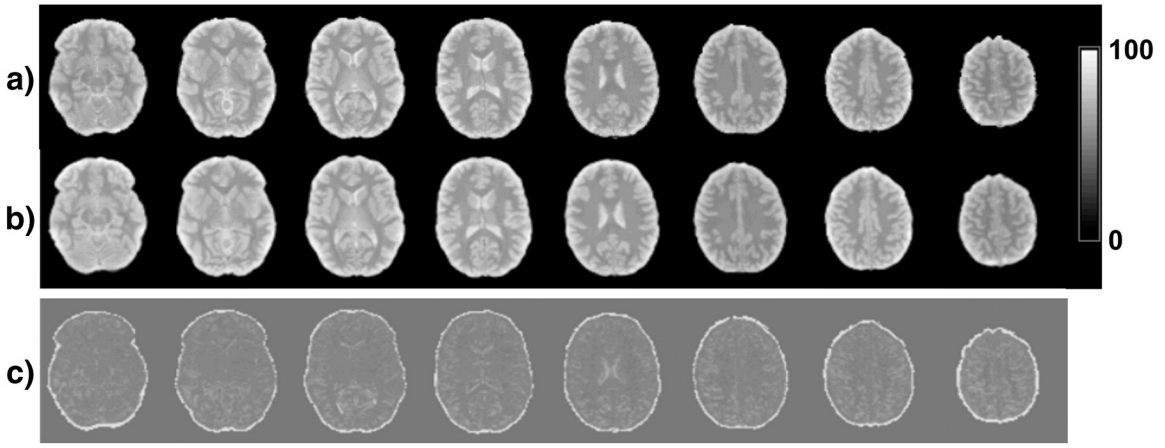

Fig. 7. Eight representative slices of M0 map, showing (a) the M0 image from a single study (b) the mean-value M0 maps calculated from five repeated studies at different times obtained from a 26-year-old female with same protocol and processing steps as described in the text; and (c) the COV image, shown with a range from 0% (background) to 10% (white). Average voxel-based COV values through the whole-brain were 2.7%, 3.9%, and 5.2% for WM, GM tissues, and CSF, respectively. Notice the bright pixels around the brain (skull) showing high variability due to low SNR in the original SPGR images and suboptimal B1 estimate at the brain boundaries, where small B1 values has caused high M0 variations.

main cause of this variation lies in the partial-volume effect, the RF fields' inhomogeneities, the intrinsic T1 variability, and in the multichannel combination methods [36]. Hence, M0 measurement based on T1 mapping needs to account for several systemic errors. In most T1-dependent M0 mapping methods, if the longitudinal relaxation time is overestimated, the resulting water content is also overestimated. This may explain why Whittall et al. [9] reported high water content values for the deep GM. Even though T1 is typically correlated with tissue water content, the explicit dependence may be different for different brain regions. Nevertheless, M0 mapping on the basis of the variable flip angle approach can yield reproducible results, potentially making it suitable for use in clinical. In alignment with other studies [11,18], here, the water in the ventricular CSF is used as a reference to quantifying the "relative" water content in the brain tissues; because the amount of water concentration in pure CSF regions is a fairly reliable measure and can only be slightly affected in rare neurological disorders; although 98%–99% water content has been reported for CSF [28]. The main advantage of this approach is to avoid the complication of external references and calibration in clinical settings while providing robust and correct M0 measurements. However, such referencing approach diminishes the ability for "absolute" quantitation of the brain water concentration. While suboptimal, water concentration can be estimated using a "single" low-flip angle proton-density-weighted image after a B1 self-calibration. It would be helpful to assess the quantitative ability of such single scan approach.

Further studies are required to verify the pathologic detectability of the proposed M0 mapping method in patients with local and global mild to moderate tissue water changes and to ascertain the clinical usefulness of M0 map in different neurological disorders. The proposed M0 mapping method has been successfully used for calibration of whole-brain MR spectroscopic imaging (MRSI) data [37] by referencing to brain tissue water signal [38]. The use of a separate water density measurement based on the proposed M0 mapping [19] has addressed the potential source of MRSI calibration error in the presence of pathologies, which was demonstrated on a group of patients with mild traumatic brain injuries [37].

One limitation of the proposed B1 estimation is the need for a small flip angle SPGR signal which may not be part of the dual SPGR acquisitions if longer TR's are chosen (see Fig.1) or when experiencing large B_1^+ deviations; hence, the linear B1 estimate based on $\sin(\alpha)\approx\alpha$ will no longer hold (although shorter TR is recommended because it reduces the total scan time). Further improvements can include an independent acquisition for B_1^+ and B_1^- measurements [39,40] and calibration of both T1 and M0 in expense of extra scan time. Another limitation of this study is that the T2* effect has been ignored – *i.e.* it has assumed constant $\exp(-TE/T2^*)$ – which might lead to an underestimation of M0 in cases where there are tissue components with short T2* relaxation time. According to Whittall et al. [9], rapidly relaxing components can represent up to 15% of the tissue in WM. To address this potential error, the shortest TE possible was used and high-order shimming performed to minimize the static magnetic field inhomogeneity therefore improving T2*. In this alignment, a multi-exponential fit of T2* with very short TE's is recommended.

In summary, the experimental results from healthy volunteers' images confirmed that the proposed method enables high-resolution, SNR-optimized, and quantitation M0 maps within a clinically tolerable scan time. In comparison with existing methods, the results showed a good agreement within the expected range of accuracy and high reproducibility. The intrinsic correction for the B1 inhomogeneity and stability of a single-scan approach provided a reliable method with a flexible range of accuracy. Consequently, RF miscalibrations were reliably and conveniently compensated and the SNR was optimized for human brain imaging at 3.0 T. This allows the method to be readily used for imaging applications in clinical settings. The excellent reproducibility of the water content signal is supporting the use of this method as a robust and reliable water content measure in longitudinal studies.

6. Conclusions

A non-invasive, simple, and straight-forward method for quantitative measurement of localized water content has been presented, which is based on the linearization of dual flip angle 3D SPGR scans. Correct M0 maps with an isotropic spatial resolution of $1 \times 1 \times 1$ mm^3 that covers the entire human brain were achieved in 6:30 min. The current in vivo results clearly demonstrate that fast SPGR sequences based on the variable excitation angle approach with appropriate parameter settings and B1-adjustment steps can obtain full brain coverage M0 mapping that is suitable for neurological clinical applications.

Acknowledgments

This research is supported by the National Institutes of Health (Grant: R01EB000822). The authors gratefully acknowledge discussions with Sang H Lee, MSc, Noam Alperin, PhD, and Sudarshan Ranganathan, MSc.

References

[1] Ludemann L, Warmuth C, Plotkin M, Forschler A, Gutberlet M, Wust P, Amthauer H. Brain tumor perfusion: comparison of dynamic contrast enhanced magnetic resonance imaging using T1, T2, and T2* contrast, pulsed arterial spin labeling, and H2(15)O positron emission tomography. Eur J Radiol 2009;70(3):465–74.

[2] Besson JA. Are NMR, brain changes in chronic alcoholism related to water content or structuring? Alcohol Clin Exp Res 1990;14(6):952–3.

[3] Laule C, Vavasour IM, Moore GR, Oger J, Li DK, Paty DW, MacKay AL. Water content and myelin water fraction in multiple sclerosis. A T2 relaxation study. J Neurol 2004;251(3):284–93.

[4] Gideon P, Rosenbaum S, Sperling B, Petersen P. MR-visible brain water content in human acute stroke. Magn Reson Imaging 1999;17(2):301–4.

[5] Shah NJ, Neeb H, Kircheis G, Engels P, Haussinger D, Zilles K. Quantitative cerebral water content mapping in hepatic encephalopathy. Neuroimage 2008;41(3):706–17.

[6] Badaut J, Lasbennes F, Magistretti PJ, Regli L. Aquaporins in brain: distribution, physiology, and pathophysiology. J Cereb Blood Flow Metab 2002;22(4):367–78.

[7] Wick W, Kuker W. Brain edema in neurooncology: radiological assessment and management. Onkologie 2004;27(3):261–6.

[8] Pauleit D, Floeth F, Hamacher K, Riemenschneider MJ, Reifenberger G, Muller HW, Zilles K, Coenen HH, Langen KJ. O-(2-[18 F]fluoroethyl)-L-tyrosine PET combined with MRI improves the diagnostic assessment of cerebral gliomas. Brain 2005;128(Pt 3):678–87.

[9] Whittall KP, MacKay AL, Graeb DA, Nugent RA, Li DK, Paty DW. In vivo measurement of T2 distributions and water contents in normal human brain. Magn Reson Med 1997;37(1):34–43.

[10] Neeb H, Zilles K, Shah NJ. A new method for fast quantitative mapping of absolute water content in vivo. Neuroimage 2006;31(3):1156–68.

[11] Volz S, Noth U, Deichmann R. Correction of systematic errors in quantitative proton density mapping. Magn Reson Med 2012;68(1):74–85.

[12] Venkatesan R, Lin W, Haacke EM. Accurate determination of spin-density and T1 in the presence of RF-field inhomogeneities and flip-angle miscalibration. Magn Reson Med 1998;40(4):592–602.

[13] Warntjes JB, Dahlqvist O, Lundberg P. Novel method for rapid, simultaneous T1, T*2, and proton density quantification. Magn Reson Med 2007;57(3):528–37.

[14] Neeb H, Ermer V, Stocker T, Shah NJ. Fast quantitative mapping of absolute water content with full brain coverage. Neuroimage 2008;42(3):1094–109.

[15] Deoni SC, Rutt BK, Peters TM. Rapid combined T1 and T2 mapping using gradient recalled acquisition in the steady state. Magn Reson Med 2003;49(3):515–26.

[16] Preibisch C, Deichmann R. T1 mapping using spoiled FLASH-EPI hybrid sequences and varying flip angles. Magn Reson Med 2009;62(1):240–6.

[17] Wang J, Qiu M, Constable RT. In vivo method for correcting transmit/receive nonuniformities with phased array coils. Magn Reson Med 2005;53(3):666–74.

[18] Gasparovic C, Neeb H, Feis DL, Damaraju E, Chen H, Doty MJ, South DM, Mullins PG, Bockholt HJ, Shah NJ. Quantitative spectroscopic imaging with in situ measurements of tissue water T1, T2, and density. Magn Reson Med 2009;62(3):583–90.

[19] Sabati M, Maudsley AA. SNR-optimized, fast, and high-resolution mapping of whole brain tissue water content. Proc 19th ISMRM. Montreal, QC, Canada; 2011. p. 2378.

[20] Wansapura JP, Holland SK, Dunn RS, Ball Jr WS. NMR relaxation times in the human brain at 3.0 tesla. J Magn Reson Imaging 1999;9(4):531–8.

[21] Helms G, Dathe H, Dechent P. Quantitative FLASH MRI at 3 T using a rational approximation of the Ernst equation. Magn Reson Med 2008;59(3):667–72.

[22] Deoni SC, Peters TM, Rutt BK. Determination of optimal angles for variable nutation proton magnetic spin–lattice, T1, and spin–spin, T2, relaxation times measurement. Magn Reson Med 2004;51(1):194–9.

[23] Weiskopf N, Lutti A, Helms G, Novak M, Ashburner J, Hutton C. Unified segmentation based correction of R1 brain maps for RF transmit field inhomogeneities (UNICORT). Neuroimage 2011;54(3):2116–24.

[24] Sabati M, Maudsley AA. Clinically-driven fast and high-resolution mapping of T1, M0, and B1 with whole brain coverage. Proc 18th ISMRM. Stockholm, Sweden; 2010. p. 2317.

[25] Smith SM. Fast robust automated brain extraction. Hum Brain Mapp 2002;17(3):143–55.

[26] Zhang Y, Brady M, Smith S. Segmentation of brain MR images through a hidden Markov random field model and the expectation–maximization algorithm. IEEE Trans Med Imaging 2001;20(1):45–57.

[27] Kreis R, Ernst T, Ross BD. Development of the human brain: in vivo quantification of metabolite and water content with proton magnetic resonance spectroscopy. Magn Reson Med 1993;30(4):424–37.

[28] Johanson CE, Duncan 3rd JA, Klinge PM, Brinker T, Stopa EG, Silverberg GD. Multiplicity of cerebrospinal fluid functions: new challenges in health and disease. Cerebrospinal Fluid Res 2008;5:10.

[29] Fleysher R, Fleysher L, Liu S, Gonen O. TriTone: a radiofrequency field (B1)-insensitive T1 estimator for MRI at high magnetic fields. Magn Reson Imaging 2008;26(6):781–9.

[30] Ordidge RJ, Gibbs P, Chapman B, Stehling MK, Mansfield P. High-speed multislice T1 mapping using inversion-recovery echo-planar imaging. Magn Reson Med 1990;16(2):238–45.

[31] Shah NJ, Neeb H, Zaitsev M, Steinhoff S, Kircheis G, Amunts K, Haussinger D, Zilles K. Quantitative T1 mapping of hepatic encephalopathy using magnetic resonance imaging. Hepatology 2003;38(5):1219–26.

[32] Deichmann R. Fast high-resolution T1 mapping of the human brain. Magn Reson Med 2005;54(1):20–7.

[33] Wright PJ, Mougin OE, Totman JJ, Peters AM, Brookes MJ, Coxon R, Morris PE, Clemence M, Francis ST, Bowtell RW, et al. Water proton T1 measurements in brain tissue at 7, 3, and 1.5 T using IR-EPI, IR-TSE, and MPRAGE: results and optimization. MAGMA 2008;21(1–2):121–30.

[34] Gowland P, Mansfield P. Accurate measurement of T1 in vivo in less than 3 seconds using echo-planar imaging. Magn Reson Med 1993;30(3):351–4.

[35] Steinhoff S, Zaitsev M, Zilles K, Shah NJ. Fast T(1) mapping with volume coverage. Magn Reson Med 2001;46(1):131–40.

[36] Trzasko JD, Mostardi PM, Riederer SJ, Manduca A. Estimating T1 from multichannel variable flip angle SPGR sequences. Magn Reson Med 2013;69(6):1787–94.

[37] Sabati M, Govind V, Maudsley AA. Signal normalization for MR spectroscopic imaging using brain tissue water: variability and pathologic detectability. Proc 19th ISMRM. Montreal, QC, Canada; 2011. p. 1434.

[38] Christiansen P, Henriksen O, Stubgaard M, Gideon P, Larsson HB. In vivo quantification of brain metabolites by 1H-MRS using water as an internal standard. Magn Reson Imaging 1993;11(1):107–18.

[39] Voigt T, Nehrke K, Doessel O, Katscher U. T1 corrected B1 mapping using multi-TR gradient echo sequences. Magn Reson Med 2010;64(3):725–33.

[40] Yarnykh VL. Actual flip-angle imaging in the pulsed steady state: a method for rapid three-dimensional mapping of the transmitted radiofrequency field. Magn Reson Med 2007;57(1):192–200.